International Journal of Mathematics and Computer Research

ISSN: 2320-7167

Volume 10 Issue 06 June 2022, Page no. – 2705-2715

Index Copernicus ICV: 57.55, Impact Factor: 7.362

DOI: 10.47191/ijmcr/v10i6.02

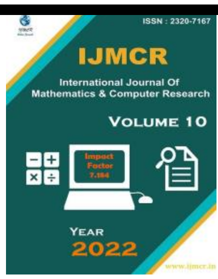

Effect of Stenotic Height on Lipid Concentrated Blood Flow through a Microchannel in The Presence of Magnetic Field

K. W. Bunonyo[1], L. Ebiwareme,G.D.Eli[3]

[1] MMDARG, Department of Mathematics and Statistics, Federal University Otuoke, Nigeria

Department of Mathematics, Rivers State University, Nigeria

[3] Department of Petroleum and Gas Engineering, Federal University Otuoke, Nigeria

ARTICLE INFO

Published Online:
04 June 2022

Corresponding Author:
K. W. Bunonyo

ABSTRACT

In this article, we develop mathematical models for blood momentum, energy equation with lipid concentration, and lipid concentration equation, all of which are subjected to an oscillatory boundary at the channel's upper wall. Using the oscillatory conditions, the governing models were scaled to a set of dimensionless models and reduced to an ordinary differential equation.

The reduced perturbed equations were directly solved, yielding blood velocity, temperature, and lipid concentration profiles. Using Wolfram Mathematica, version 10, the obtained flow profiles were coded by varying some of the important biophysical parameters.

Conclusively, it is noticed that the thermal Grashof number and solutal Grashof number increase caused the blood velocity to increase; the concentration source parameter increase also increased the blood velocity. Furthermore, the velocity decreases with the increase in the Hartman and Schmidt numbers, respectively. Further investigation revealed that increasing the height of stenosis and lipid source parameter increases the temperature profile, but increasing radiation absorption, Prandtl number, oscillatory frequency, and womersley number decreases the temperature of the fluid. These findings are of great interest to mathematicians, physicists, and other researchers working on blood flow issues and the development of medical prosthetic devices.

KEYWORDS: Blood, Circulation, Stenosis, Mathematical Formulation, Lipid, Concentration, Biomagnetic, Microchannel.

1. INTRODUCTION

The circulatory system is made up of the heart, blood, and blood vessels. The heart is a muscle that never stops beating and is pulsatile in nature; it pumps blood around the body. The left side pumps oxygen and nutrient rich blood to the brain, muscles, organs, and every cell in the body. The right side of the heart is slightly smaller and returns blood to the lungs to be topped up with oxygen. The heart has its own blood supply, which comes from the coronary arteries. According to Bunonyo and Amos (2020), these divide many times to provide oxygen and nutrients to every part of the heart muscle to help keep it healthy and pumping normally.

According to the NHS review, (2019), heart disease occurs when any of the vessels in the body (arteries) becomes narrow due to the slow build-up of fatty material (called plaque or atheroma), in a process called atherosclerosis. It causes coronary heart disease (CHD). Sometimes an artery can become so narrow it cannot deliver sufficient blood to the body's needs. This results in warning symptoms such as chest pain, called stable angina. When these fatty deposits become very large or extended, they may burst, and a blood clot and then scarring form over the damaged area. Over time, this damage may partly or completely block the artery. When this happens, it is called acute coronary syndrome (ACS), unstable angina or heart attack. A heart attack is sometimes referred to as a myocardial infarction, or MI.

According to Bunonyo and Amos (2020), atherosclerosis is a very slow process, happening over many years. It can start very early in life and results in the buildup of fatty material in the linings of the blood vessels. These fatty deposits start when the blood vessel lining becomes damaged. This makes it easier for cholesterol (carried on lipoproteins like LDL) to stick on and build up more rapidly. However, HDL lipoproteins can remove cholesterol from these deposits. Reducing your LDL cholesterol, increasing your HDL cholesterol, and reducing other risk factors can help slow down the process of atherosclerosis. See below the figure showing a blood vessel with plaque buildup. According to Okpeta and Bunonyo (2021), hardening of the arteries results in atherosclerosis and restricts normal blood flow because of the loss of vessel flexibility. The heart works harder to push blood through to the downstream.

Biomagnetic fluid dynamics has many major applications, such as magnetic drug targeting, adjusting blood flow during surgery, transporting complex bio-waste fluids, cancer tumor treatment, etc. Extensive research has been undertaken on the fluid dynamics of bio-magnetic fluids under the presence of an external magnetic field. The application of magneto-hydrodynamics in physiological flow is of growing interest as many researchers have reported that blood is an electrically conducting fluid, Rathee and Singh (2010) Over several decades, there have been so many researchers that have worked on blood flow problems; a mathematical modeling of tumor growth in mice following low-level direct electric current was proposed by Cabrales *et al.* (2008). There are many other researchers that have worked on researchers related to blood flow through an artery. They are as follows: Bonate (2011) modeled tumor growth in oncology, where oncology is the study of cancer. He developed mathematical models of preclinical and clinical tumor growth. Makinde *et al*. (2006) studied the blood vessels formed in asthmatic airways that are involved in inflammatory and airway remodeling processes in chronic asthma. Mandel (2005) investigated an unsteady analysis of non-Newtonian blood through the tapered arteries with stenosis. The non-Newtonian blood flow problem was solved numerically with the finite difference scheme used to solve the unsteady nonlinear Navier-Stokes equation in the cylindrical coordinate system governing flow with verifiable assumptions to reduce the problem to two-dimensional flow. Zhu *et al*. (2012) researched on tumor growth under hyperthermia conditions and came to the conclusion with both the tumor growth rate curve and corresponding average glucose concentration and obtained numerical results illustrating the controlling effect on tumor growth under hyperthermia conditions in the initial stage. Makinde and Osalusi (2006) researched the hydromagnetic steady flow of a viscous conducting fluid in a channel with slip at the permeable boundaries. An analytical solution was gotten for the governing nonlinear boundary values problem using the perturbation method together with a pade approximation technique based on computer extended series solution and their results. However, to the best of our knowledge, none of the aforementioned researchers were able to talk about the impact of lipid concentration on thermal energy as well as on blood momentum. Secondly, no one of the aforementioned researchers talked about the growth of stenosis and how it affects the energy generated that affects the blood thickness as well as the circulation of the fluid, except Bunonyo and Amadi (2021), who discussed just the velocity profile without considering the energy impact, and Bunonyo and Ebiwareme (2022), who discussed the effect of the temperature profile on the velocity distribution, but in this present article we shall discuss the effect of the lipid concentration on the velocity profile and on temperature profile, respectively, and also look at how the height of stenosis contributes to all this.

2. MATHEMATICAL MODELS

2.1 The geometry of a stenosed microchannel

Let us consider that blood is an electrically conducting, incompressible, viscous fluid. It flows through a stenosed channel, which is assumed to be a microchannel, $w^*\left(y^*, x^*\right)$ is the velocity of the fluid, where y^* and x^* are the direction of the flow. The oscillatory flow arises due to the contraction and relaxation of the heart, the pressure gradient is in the axial direction; and the magnetic field is applied perpendicularly to the direction of the flow. The geometry of a stenosed microchannel is considered to be:

$$y^* = \begin{cases} R_0 - \delta^* cos\left(2\pi \dfrac{x^*}{\lambda^*}\right) & \text{at } 0 \le x^* \le d_0 \\ R_0 & \text{at } d_0 \le x^* \le \lambda^* \end{cases} \tag{1}$$

2.2 Governing Models

The models governing the viscous flow through a microchannel follow Bunonyo and Ebiwareme (2022), Bunonyo and Amadi (2021), Bunonyo and Eli (2020), Misra and Adhikary (2016), Eldesoky (2013), where we modified the momentum and energy equation and introduced the particles concentration in the fluid and formed autonomous concentration equation, and present them as follows:

2.2.1 Momentum Equation

$$\frac{\partial w^*}{\partial t^*}+V_0\left(1+\varepsilon e^{i\omega t}\right)\frac{\partial w^*}{\partial y^*}=\frac{1}{\rho_b}\frac{\partial P^*}{\partial x^*}+\upsilon\frac{\partial^2 w^*}{\partial y^{*2}}-\frac{\upsilon w^*}{k^*}-\sigma\frac{B_0^2 w^*}{\rho_b}+g\beta_T\left(T-T_a\right)+g\beta_C\left(C-C_a\right) \quad (2)$$

2.2.2 Energy Equation

$$\rho_b c_b\frac{\partial T^*}{\partial t^*}=k_b\frac{\partial^2 T^*}{\partial y^{*2}}-\rho_a\rho_b w_b\left(T-T_a\right)+S\left(C-C_a\right) \quad (3)$$

2.2.3 Lipid Concentration Equation

$$\frac{\partial C^*}{\partial t^*}=D_m\frac{\partial^2 C^*}{\partial y^{*2}}-k_c\left(C-C_a\right) \quad (4)$$

The boundary conditions follow those in Bunonyo and Amos (2020), The boundary conditions are:

$$\left.\begin{array}{ll}\frac{\partial w^*}{\partial y^*}=0,\frac{\partial T^*}{\partial y^*}=0,\frac{\partial C^*}{\partial y^*}=0 & \text{at} \quad y^*=0 \\ w^*=0,T^*=T_a+\left(T_w-T_a\right)e^{i\omega t},C^*=C_a+\left(C_w-C_a\right)e^{i\omega t} & \text{at} \quad y^*=R\end{array}\right\} \quad (5)$$

3. DIMENSIONAL VARIABLES

We introduce the following dimensionless parameters:

$$\left.\begin{array}{l} y=\frac{y^*}{R_0},x=\frac{x^*}{\lambda},\lambda=\frac{\lambda^*}{R_0},\delta=\frac{\delta^*}{R_0},w=\frac{w^*}{\upsilon w_0},P=\frac{P^*R_0^2}{\mu\lambda w_0},\theta=\frac{T-T_a}{T_w-T_a},Rd_c=\frac{k_cR_0^2}{\upsilon} \\ Rd_1=\frac{R_0^2\rho_a\rho_bF}{\mu_bc_b},Gr=\frac{g\beta_{Tb}\left(T_w-T_a\right)R_0^2}{\upsilon^2w_0},\frac{R_0^2}{k^*}=\frac{1}{k},Re=\frac{V_0R_0}{\upsilon},\alpha^2=\frac{\rho_bR_0^2\omega}{\mu}, \\ M^2=\frac{\sigma B_0^2R_0^2}{\mu},t=\omega t^*,Pr=\frac{\mu_bc_b}{k_b},S_1=\frac{R_0^2S\left(t\right)}{k_b\left(T_w-T_a\right)},Sc=\frac{\upsilon}{D_m},\phi=\frac{C-C_a}{C_w-C_a}\end{array}\right\} \quad (6)$$

Using the dimensionless variables in equation (6), equations (2)-(5) reduced to:

$$\alpha^2\frac{\partial w}{\partial t}+Re\frac{\partial w}{\partial y}=\frac{\partial P}{\partial x}+\frac{\partial^2 w}{\partial y^2}-\frac{w}{k}-M^2w+Gr\theta+Gc\phi \quad (7)$$

$$\alpha^2Pr\frac{\partial\theta}{\partial t}=\frac{\partial^2\theta}{\partial y^2}-Rd_1Pr\theta+S_1 \quad (8)$$

$$\alpha^2Sc\frac{\partial\phi}{\partial t}=\frac{\partial^2\phi}{\partial y^2}-Rd_2Sc\phi \quad (9)$$

where $\varepsilon=0$

The geometry of the stenosed region at the upper wall is:

$$y=\begin{cases}1-\delta cos\left(2\pi x\right) & \text{at} \quad 0\le x\le\frac{d_0}{\lambda} \\ 1 & \text{at} \quad \frac{d_0}{\lambda}\le x\le R_0\end{cases} \quad (10)$$

The corresponding boundary conditions are

$$\left.\begin{array}{lll}\frac{\partial w}{\partial y}=0,\theta=0,\phi=0 & \text{at} & y=0\\ w=0,\theta=e^{i\omega t},\phi=e^{i\omega t} & \text{at} & y=1-\delta cos\left(2\pi x\right)\end{array}\right\} \tag{11}$$

4. METHOD OF SOLUTION

Since the flow is due to the contraction and relaxation of the heart, we consider the oscillatory solution to be in the following form:

$$\left.\begin{array}{l}w\left(y,t\right)=w_1\left(y\right)e^{i\omega t},\theta\left(y,t\right)=\theta_1\left(y\right)e^{i\omega t}\\ \phi\left(y,t\right)=\phi_1\left(y\right)e^{i\omega t},S_1=S_2e^{i\omega t},-\frac{\partial P}{\partial x}=P_1e^{i\omega t}\end{array}\right\} \tag{12}$$

In order to reduce the governing equations to ordinary differential equations; we substitute equation (12) into equations (8)-(9), we have

$$\frac{\partial^2\phi_1}{\partial y^2}-\beta_1^2\phi_1=0 \tag{13}$$

$$\frac{\partial^2\theta_1}{\partial y^2}-\beta_2^2\theta_1=-S_2 \tag{14}$$

where $\beta_1^2=\left(Rd_2+\alpha^2 i\omega\right)Sc$ and $\beta_2^2=\left(Rd_1+\alpha^2 i\omega\right)Pr$

Solving equations (13) and (14), we have:

$$\phi_1\left(y\right)=A_1 sinh\left(\beta_1 y\right)+B_1 cosh\left(\beta_1 y\right) \tag{15}$$

$$\theta_1\left(y\right)=A_2 sinh\left(\beta_2 y\right)+B_2 cosh\left(\beta_2 y\right)+\frac{S_2}{\beta_2^2} \tag{16}$$

Substituting equation (12) into equation (11), we have the boundary conditions as:

$$\left.\begin{array}{lll}w_1=0,\theta_1=1,\phi_1=1 & \text{at} & y=h\equiv 1-\delta cos\left(2\pi x\right)\\ \frac{\partial w_1}{\partial y}=0,\frac{\partial\theta_1}{\partial y}=0,\frac{\partial\phi_1}{\partial y}=0 & \text{at} & y=0\end{array}\right\} \tag{17}$$

Solving equations (15) and (16) subjecting the boundary conditions in equation (17), we have:

$$\phi_1\left(y\right)=\frac{cosh\left(\beta_1 y\right)}{cosh\left(\beta_1 h\right)} \tag{18}$$

$$\theta_1\left(y\right)=\frac{S_2}{\beta_2^2}+\left(1-\frac{S_2}{\beta_2^2}\right)\frac{cosh\left(\beta_2 y\right)}{cosh\left(\beta_2 h\right)} \tag{19}$$

Substituting equation (12) into equation (7), we have

$$\frac{\partial^2 w_1}{\partial y^2}-Re\frac{\partial w_1}{\partial y}-\beta_3^2 w_1=-P_1-Gr\theta_1-Gc\phi_1 \tag{20}$$

where $\beta_3^2=\left(\frac{1}{k}+M^2+\alpha^2 i\omega\right)$

Substitute equations (18) and (19) into equation (20), we have

$$\frac{\partial^2 w_1}{\partial y^2}-Re\frac{\partial w_1}{\partial y}-\beta_3^2 w_1=-P_2-\phi_2 cosh\left(\beta_2 y\right)-\phi_3 cosh\left(\beta_1 y\right) \tag{21}$$

where $P_2=\left(P_1+\frac{S_2 Gr}{\beta_2^2}\right),\phi_2=\left(\left(1-\frac{S_2}{\beta_2^2}\right)\frac{Gr}{cosh\left(\beta_2 h\right)}\right),\phi_3=\left(\frac{Gc}{cosh\left(\beta_1 h\right)}\right)$

The homogenous solution of equation (21) is

$$w_c(y) = A_3 e^{m_1 y} + B_3 e^{m_2 y} \tag{22}$$

where $\alpha_1 = Re$, $m_1 = \dfrac{\alpha_1 + \sqrt{\alpha_1^2 + 4\beta_3^2}}{2}$ and $m_2 = \dfrac{\alpha_1 - \sqrt{\alpha_1^2 + 4\beta_3^2}}{2}$

The particular solution of equation (21) is

$$w_p(y) = A_4 + A_5 cosh(\beta_2 y) + A_6 cosh(\beta_1 y) \tag{23}$$

The solution to equation (21) is

$$w_1(y) = A_3 e^{m_1 y} + B_3 e^{m_2 y} + A_4 + A_5 cosh(\beta_2 y) + A_6 cosh(\beta_1 y) \tag{24}$$

where $A_5 = \dfrac{\phi_2}{(\beta_3^2 - \beta_2^2)}, A_6 = \dfrac{\phi_3}{(\beta_3^2 - \beta_1^2)}, A_4 = \dfrac{P_2}{\beta_3^2}$

Solving equation (24) using the boundary condition in equation (12), we have

$$A_3 m_1 + B_3 m_2 = 0, \tag{25}$$

$$A_3 e^{m_1 h} + B_3 e^{m_2 h} = \phi_4, \tag{26}$$

where $\phi_4 = -A_4 - A_5 cosh(\beta_2 h) - A_6 cosh(\beta_1 h)$

Equations (25)-(26) can be presented as:

$$\begin{pmatrix} m_1 & m_2 \\ e^{m_1 h} & e^{m_2 h} \end{pmatrix} \begin{pmatrix} A_3 \\ B_3 \end{pmatrix} = \begin{pmatrix} 0 \\ \phi_4 \end{pmatrix} \tag{27}$$

where the solution to equation (27) is

$$A_3 = \frac{-\phi_4 m_2}{m_1 e^{m_2 h} - m_2 e^{m_1 h}}, B_3 = \frac{m_1 \phi_4}{m_1 e^{m_2 h} - m_2 e^{m_1 h}} \tag{28}$$

Substituting equation (28) into equation (4), we have

$$w(y,t) = \left(\left(\frac{-\phi_4 m_2}{m_1 e^{m_2 h} - m_2 e^{m_1 h}} \right) e^{m_1 y} + \left(\frac{m_1 \phi_4}{m_1 e^{m_2 h} - m_2 e^{m_1 h}} \right) e^{m_2 y} + A_4 + A_5 cosh(\beta_2 y) + A_6 cosh(\beta_1 y) \right) e^{i\omega t}$$

(29)

5. RESULTS

This research is an extension of previous by Bunonyo and Ebiwareme (2022), Bunonyo and Amadi (2021), where we introduced lipid concentration on the energy equation and considered it also on the momentum equation. The formulated equations were solved comprehensively. The obtained analytical solutions were coded using Wolfram Mathematica, version 12, and the useful parameters were varied to study the effects of aforementioned parameters on the flow profiles. The results are as follows:

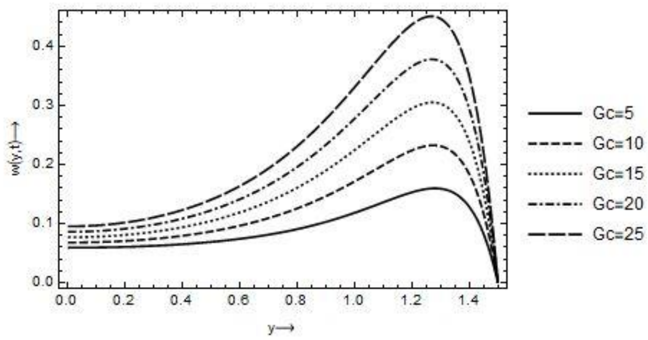

Fig 1: Effect of solutal Grashof number on velocity, with $Gr = 15, Pr = 21, Rd_1 = 3, S_2 = 2, M = 3, Sc = 2$ $Rd_2 = 2, Re = 2, \alpha = 2, \delta = 0.5, k = 0.05, \omega = 0.4$

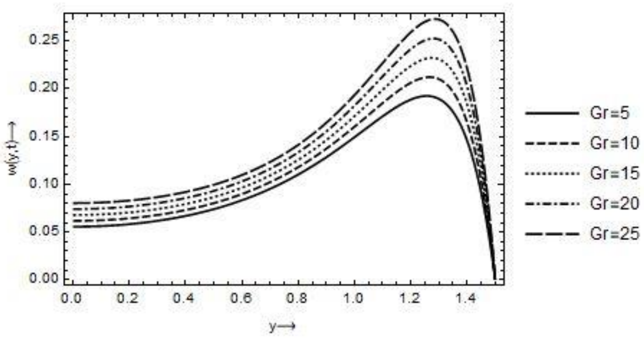

Fig 2: Effect of Grashof number on velocity, with $Gc = 10, Pr = 21, Rd_1 = 2, S_2 = 2, M = 3, Sc = 2$ $Rd_2 = 3, Re = 2, \alpha = 2, \delta = 0.5, k = 0.05, \omega = 0.4$

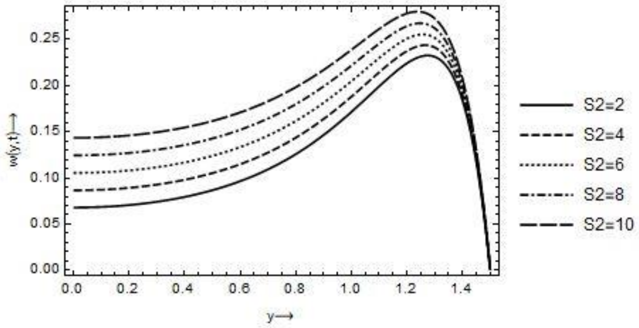

Fig 3: Effect of lipid source on concentration, with
$$Gc=10, Pr=21, Rd_1=2, Gr=15, M=3, Sc=2$$
$$Rd_2=2, Re=2, \alpha=2, \delta=0.5, k=0.05, \omega=0.4$$

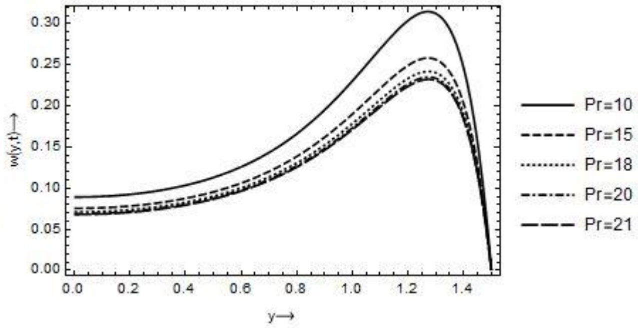

Fig 4: Effect of Prandtl number on velocity, with
$$Gr=10, Gc=15, Rd_1=2, S_2=2, M=3, Sc=2$$
$$Rd_2=3, Re=2, \alpha=2, \delta=0.5, k=0.05, \omega=0.4$$

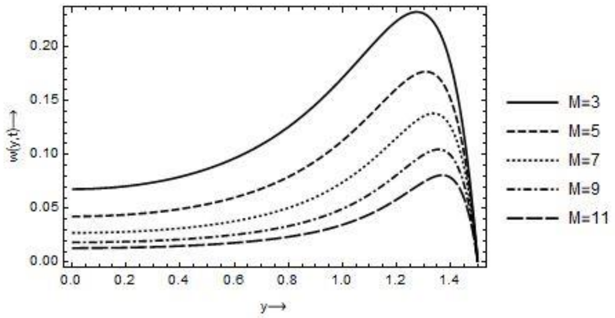

Fig 5: Effect of Hartmann number on velocity, with
$$Gr=10, Pr=21, Rd_1=2, S_2=2, Gc=15, Sc=2$$
$$Rd_2=3, Re=2, \alpha=2, \delta=0.5, k=0.05, \omega=0.4$$

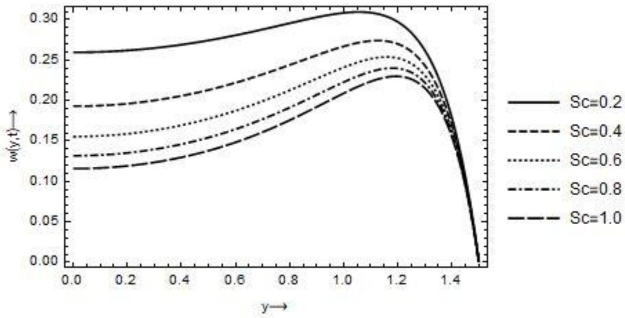

Fig 6: Effect of Schmidt number on velocity, with
$$Gr=10, Pr=21, Rd_1=2, S_2=2, M=3, Gc=15$$
$$Rd_2=3, Re=2, \alpha=2, \delta=0.5, k=0.05, \omega=0.4$$

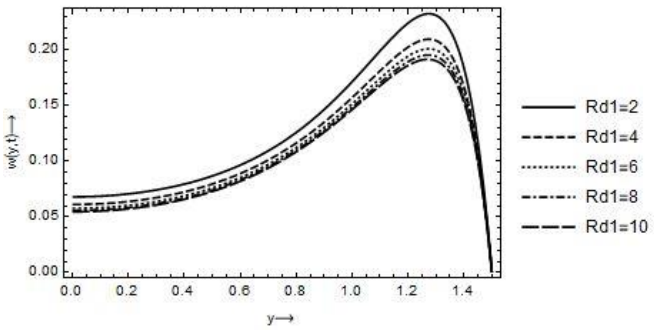

Fig 7: Effect of radiation absorption on velocity, with
$$Gr=10, Pr=21, Gc=15, S_2=2, M=3, Sc=2$$
$$Rd_2=3, Re=2, \alpha=2, \delta=0.5, k=0.05, \omega=0.4$$

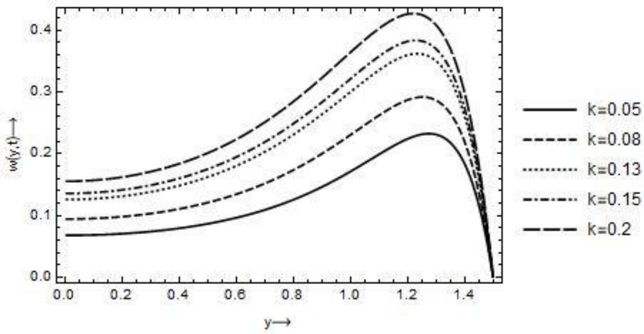

Fig 8: Effect of Darcy number on velocity, with
$$Gr=10, Pr=21, Rd_1=2, S_2=2, M=3, Sc=2$$
$$Rd_2=3, Re=2, \alpha=2, \delta=0.5, Gc=15, \omega=0.4$$

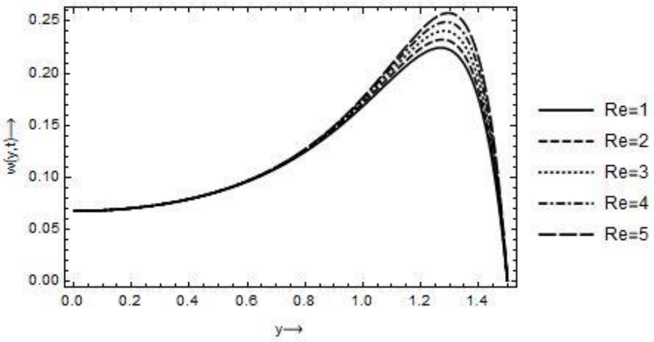

Fig 9: Effect of Reynolds number on velocity, with $Gr=10, Pr=21, Rd_1=2, S_2=2, M=3, Sc=2$ $Rd_2=3, Gc=15, \alpha=2, \delta=0.5, k=0.05, \omega=0.4$

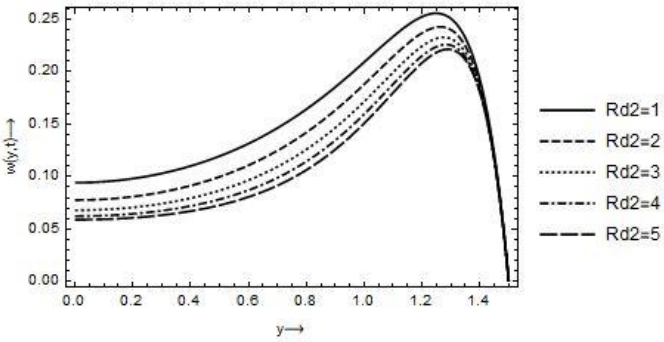

Fig 10: Effect of chemical reaction on velocity, with $Gr=10, Pr=21, Rd_1=2, S_2=2, M=3, Sc=2$ $Gc=15, Re=2, \alpha=2, \delta=0.5, k=0.05, \omega=0.4$

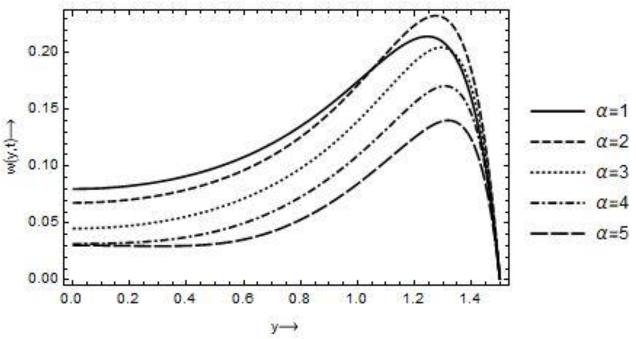

Fig 11: Effect of womersley number on velocity, with $Gr=10, Pr=21, Rd_1=2, S_2=2, M=3, Sc=2$ $Rd_2=3, Re=2, Gc=15, \delta=0.5, k=0.05, \omega=0.4$

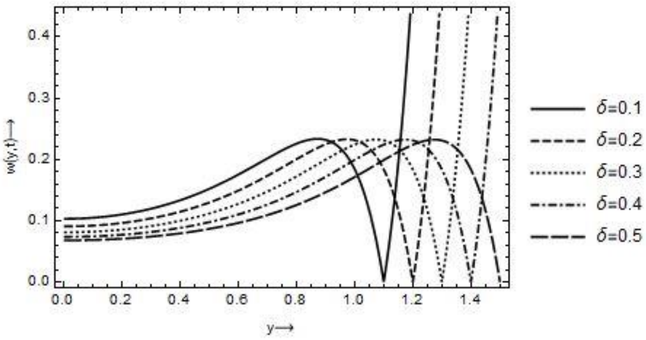

Fig 12: Effect of stenotic height on velocity, with $Gr=10, Pr=21, Rd_1=2, S_2=2, M=3, Sc=2$ $Rd_2=3, Re=2, \alpha=2, Gc=15, k=0.05, \omega=0.4$

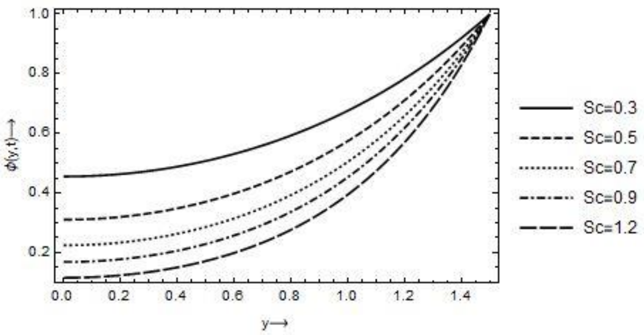

Fig 13: Effect of Schmidt number on concentration, with $Rd_2=3, \delta=0.5, \alpha=2, \omega=0.04$

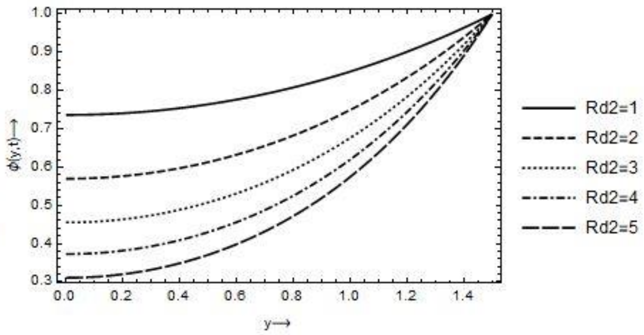

Fig 14: Effect of chemical reaction on concentration, with $Sc=0.3, \delta=0.5, \alpha=2, \omega=0.04$

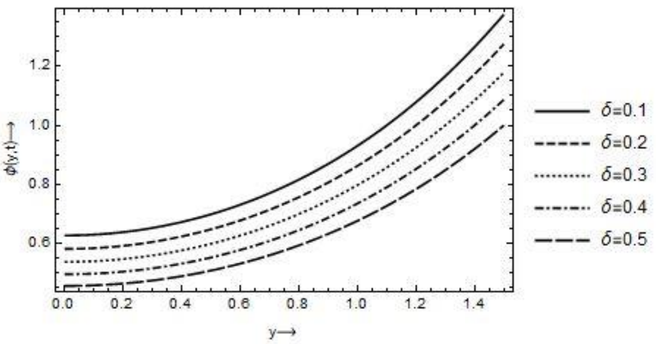

Fig 15: Effect of stenotic height on concentration, with $Rd_2=3, Sc=0.3, \delta=0.5, \omega=0.04$

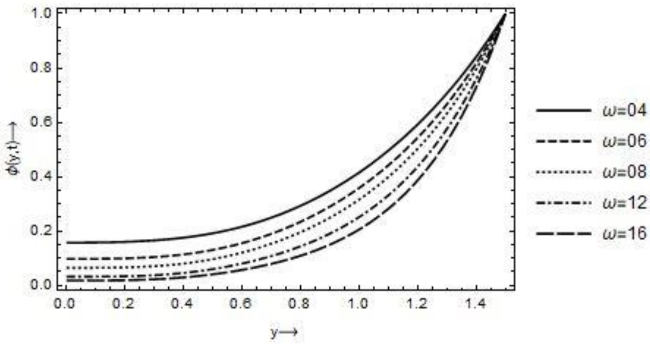

Fig 16: Effect of oscillatory frequency on concentration, with $Rd_2=3, Sc=0.3, \delta=0.5, \alpha=2$

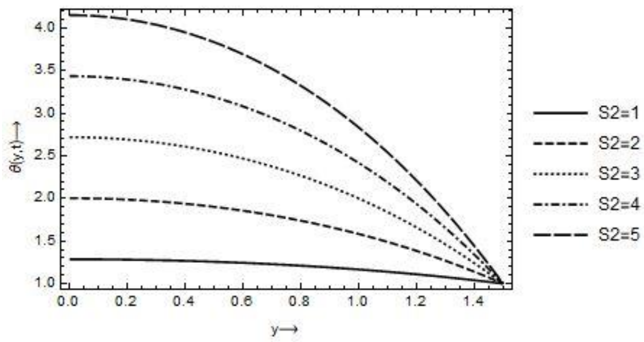

Fig 17: Effect of lipid source on concentration, with
$Rd_1 = 2, Pr = 0.3, \delta = 0.5, \omega = 0.04, \alpha = 2$

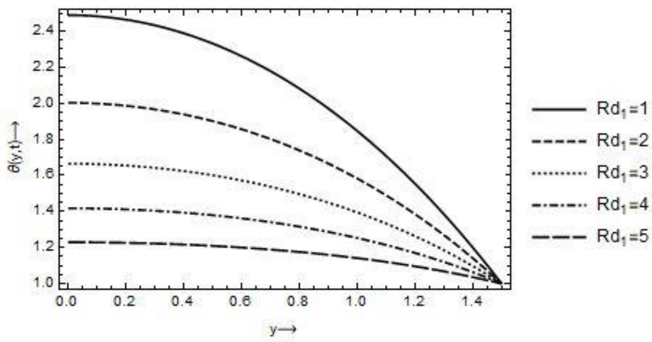

Fig 18: Effect of radiation absorption on temperature, with
$S_2 = 2, Pr = 0.3, \delta = 0.5, \omega = 0.04, \alpha = 2$

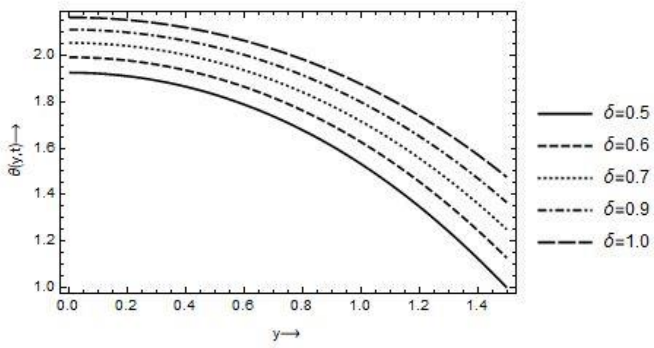

Fig 19: Effect of stenotic height on temperature, with
$Rd_1 = 2, Pr = 0.3, S_2 = 2, \omega = 0.04, \alpha = 2$

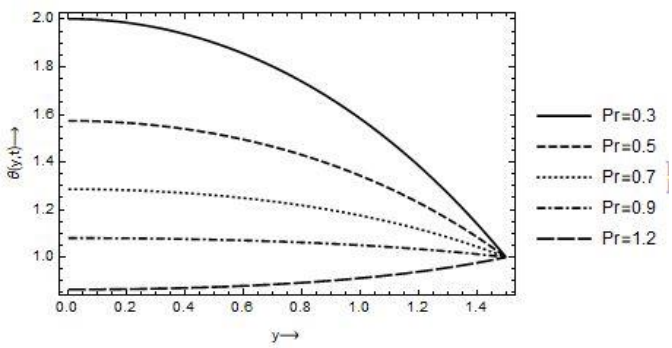

Fig 20: Effect of Prandtl number on temperature, with
$Rd_1 = 2, S_2 = 2, \delta = 0.5, \omega = 0.04, \alpha = 2$

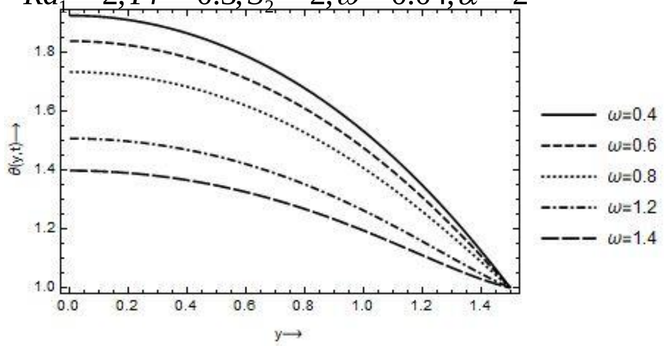

Fig 21: Effect of oscillatory frequency on temperature, with
$Rd_1 = 2, Pr = 0.3, \delta = 0.5, S_2 = 2, \alpha = 2$

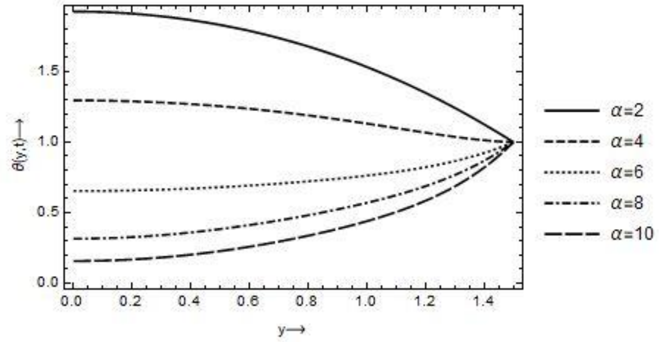

Fig 22: Effect of womersley number on temperature, with
$Rd_1 = 2, Pr = 0.3, \delta = 0.5, \omega = 0.04, S_2 = 2$

6. DISCUSSION

The aim of the research is to derive a mathematical model to investigate the blood flow through a stenosed channel with the height of the stenosis subjected to treatment and heat source. The flow profiles were obtained and Mathematica codes were developed with some entering parameters varied to see their effect on the flow. After proper formulation and solution were obtained, and the results were presented graphically, we discussed the results as follows:

Fig 1 illustrates the effect of solutal Grashof number on blood velocity, with an improving blood velocity, with an increase in Grashof number $Gc = 5, 10, 15, 20, 25$. In a similar observation, it is seen in Fig 2, that the blood velocity increases for an increase Grashof number $Gr = 5, 10, 15, 20, 25$. Fig 3 depicts that the velocity of the fluid decreases for an increasing values of the dimensionless concentration source $S_2 = 2, 4, 6, 8, 10$. However, it is seen in Fig 4 that the velocity of the fluid decreases for any increase in Prandtl number. The effect of the magnetic field was investigate as seen in Fig 5, and the result showed that the velocity profile decreases for an increase in magnetic field intensity $M = 3, 5, 7, 9, 11$. Fig 6 noted that increase in Schmidt number decreases the fluid velocity. We investigated the impact of radiation absorption on the flow and found the result in Fig 7 depicting that the velocity decreases for an increase in the radiation absorption $Rd_1 = 2, 4, 6, 8, 10$. The porosity of the channel was also investigated, and the result found showed that the velocity increases for an increasing value of the porosity $k = 0.05, 0.08, 0.13, 0.15, 0.2$. The Reynolds number effect on blood velocity was also investigated and the result in Fig 9 showed that blood velocity increases for an increasing value of the Reynolds number $Re = 1, 2, 3, 4, 5$. The chemical reaction on blood velocity was investigated and result found indicated that, the velocity decreases for an increase in reaction as depicted in Fig 10. The womersley number effect was investigated as seen in Fig 11, and this result depicts that the velocity of the fluid decreases for an increase in womersley number. The height of blood velocity was investigated as seen in Fig 12, and it elucidated that the blood velocity decreases for an increase in the height of stenosis $\delta = 0.1, 0.2, 0.3, 0.4, 0.5$ due to the excessive intake of cholesterol laden substances into the body. One of the objectives of the study is to investigate the impact of concentration level on the fluid; therefore, we are constraint to study the concentration profile for the effect of different pertinent parameters. Hence, results obtained as shown in Figs (13)-(16) indicate that increase in Schmidt number, chemical reaction height of stenosis and oscillatory frequency parameters affect the concentration profile of the fluid. In furtherance of our study, we also investigated the effect of concentration on temperature and blood velocity profiles; results in Figs (19)-(22) indicated that the temperature profile increases for an increasing value of stenotic height, Prandtl number, oscillatory frequency and womersley number.

7. CONCLUSION

This article was able to capture the impact of the concentration of lipid on the temperature profile and other pertinent parameters variation on concentration and on blood velocity. Hence, we conclude as follows:

1. It is noticed that increasing the solutal Grashof number, thermal Grashof number, and Prandtl number increases the blood velocity.
2. The study also showed that the velocity of the fluid decreases if we increase the values of the radiation absorption, magnetic field parameter, Schmidt number, radiation absorption, and chemical reaction. while the velocity increases to increase the porosity of the channel.
3. It is also seen that the velocity decreases if the womersley number and the height of stenosis increase.
4. We can easily conclude also that the concentration of the fluid decreases if the values of the Schmidt number, chemical reaction, height of stenosis, and oscillatory frequency are increased. But the increase in concentration due to an increase in stenotic height is due to the presence of constant temperature, which helps in controlling that.
5. The temperature of the fluid increases for the increasing values of the concentration source parameter, height of stenosis, Prandtl number, oscillatory frequency parameter, and womersley number, while the temperature decreases for an increasing value of radiation absorption.

REFERENCES

1. Bonate, P. L. (2011). Modeling tumor growth in oncology. *Pharmacokinetics in drug development*, 1-19.
2. Bunonyo, K. W., & Amos, E. (2020). Lipid Concentration Effect on Blood Flow Through an Inclined Arterial Channel with Magnetic Field. *Mathematical Modelling and Applications*, *5*(3), 129.
3. Bunonyo, K. W., & Ebiwareme, L. (2022). Oscillatory Blood Flow and Embolitic Plaque Effect Through a Microchannel with Metabolic Heat and Magnetic Field. *European Journal of Applied Physics*, *4*(1), 35-51.
4. Bunonyo, K. W., & Eli, I. C. (2020). Mathematical Modeling of an Oscillatory MHD Blood Flow through a Lipid Saturated Porous Channel with Metabolic Heat and Magnetic Field. *Communication in Physical Sciences*, *6*(1).
5. Bunonyo, K. W., & Amadi, C. U. (2021). Mathematical Modeling of Treatment Effect on Tumor Growth and Blood Flow through a Channel with Magnetic Field. *Journal of Advances in Mathematics and Computer Science*, *36*(7), 66-79.
6. Cabrales, L. E. B., Aguilera, A. R., Jiménez, R. P., Jarque, M. V., Ciria, H. M. C., Reyes, J. B., ... & Ávila, M. G. (2008). Mathematical modeling of tumor growth in mice following low-level direct electric current. Mathematics and Computers in Simulation, 78(1), 112-120.
7. Eldesoky, I. M. (2012). Mathematical analysis of unsteady MHD blood flow through parallel plate channel with heat source. In *The International Conference on Mathematics and Engineering Physics* (Vol. 6, No. International Conference on Mathematics and Engineering Physics (ICMEP-6), pp. 1-16). Military Technical College.
8. Makinde, O. D., & Osalusi, E. (2006). MHD steady flow in a channel with slip at the permeable boundaries. Romanian Journal of Physics, 51(3/4), 319

9. Makinde, T., Murphy, R. F., & Agrawal, D. K. (2006). Immunomodulatory role of vascular endothelial growth factor and angiopoietin-1 in airway remodeling. *Current molecular medicine*, *6*(8), 831-841.
10. Mandal, P. K. (2005). An unsteady analysis of non-Newtonian blood flow through tapered arteries with a stenosis. International Journal of Non-Linear Mechanics, 40(1), 151-164.
11. Misra, J. C., & Adhikary, S. D. (2016). MHD oscillatory channel flow, heat and mass transfer in a physiological fluid in presence of chemical reaction. *Alexandria Engineering Journal*, *55*(1), 287-297.
12. Davies O. Okpeta, K.W. Bunonyo (2021). Effect of Lipoprotein Concentration on MHD Blood flow through Parallel Plate with Heat source and Magnetic Intensity *International Journal of Mathematics Trends and Technology*, 62-80.
13. Singh, J., & Rathee, R. (2010). Analytical solution of two-dimensional model of blood flow with variable viscosity through an indented artery due to LDL effect in the presence of magnetic field. International Journal of Physical Sciences, 5(12), 1857-1868.
14. Zhu, Q., Zhang, A., Liu, P., & Xu, L. X. (2012). Study of tumor growth under hyperthermia condition. Computational and mathematical methods in medicine, 2012.
15. https://www.nhs.uk/conditions/atherosclerosis

NOMENCLATURES

w^*	Dimensional velocity component
x^*	Dimensional axial distance
y^*	Dimensional vertical distance
t^*	Dimensional time
B_0	Magnetic field
$R(x,t)$	Radius of tumor depleted region
R_0	Radius of normal arterial region
P_1	Pulsatile pressure
T_a	Arterial temperature
T^*	Dimensional temperature
C_a	Concentration at the arterial wall
C^*	Dimensional concentration
S_2	Metabolic heat generation
$w_1(y)$	Perturbed unsteady fluid velocity
$w(y,t)$	Fluid velocity profile
$\vec{B}$	Magnetic flux density
V_0	Suction velocity
S_2	Lipid source term

GREEK SYMBOLS

ν	Kinematic Viscosity of blood
μ_b	Dynamic viscosity of blood
c_b	Specific heat capacity of the fluid
k_T	Thermal conductivity of the fluid

ρ_a, ρ_b	Tissue and blood densities
g	Acceleration due to gravity
δ^*	Height of tumor growth
σ	Electrical conductivity
ω	Oscillatory frequency
λ^*	Dimensional length of atherosclerosis
θ	Dimensionless temperature of the fluid
ϕ	Dimensionless concentration in the fluid
MMDARG	Mathematical Modeling and Data Analytic Research Group